

# HEWES: Heisenberg-Euler Weak-Field Expansion Simulator

Andreas Lindner, Baris Ölmez, Hartmut Ruhl

*Arnold Sommerfeld Center for Theoretical Physics, Ludwig-Maximilians-Universität München  
Theresienstr. 37, D-80333 München, Germany*

## Abstract

A numerical simulation code of nonlinear effective light-light interactions in the weak-field expansion of the famous Heisenberg-Euler theory of quantum electrodynamics is presented. The field of application is the quantum vacuum, where these interactions can be triggered by high-intensity laser pulse collisions, causing a variety of intriguing effects. Since theoretical approaches are limited to approximations and manageable configurations, and the experimental requirements for the detection of these signals are high, the need for support from the numerical side is apparent.

*Keywords:* quantum vacuum, Heisenberg-Euler, simulations, nonlinear interactions

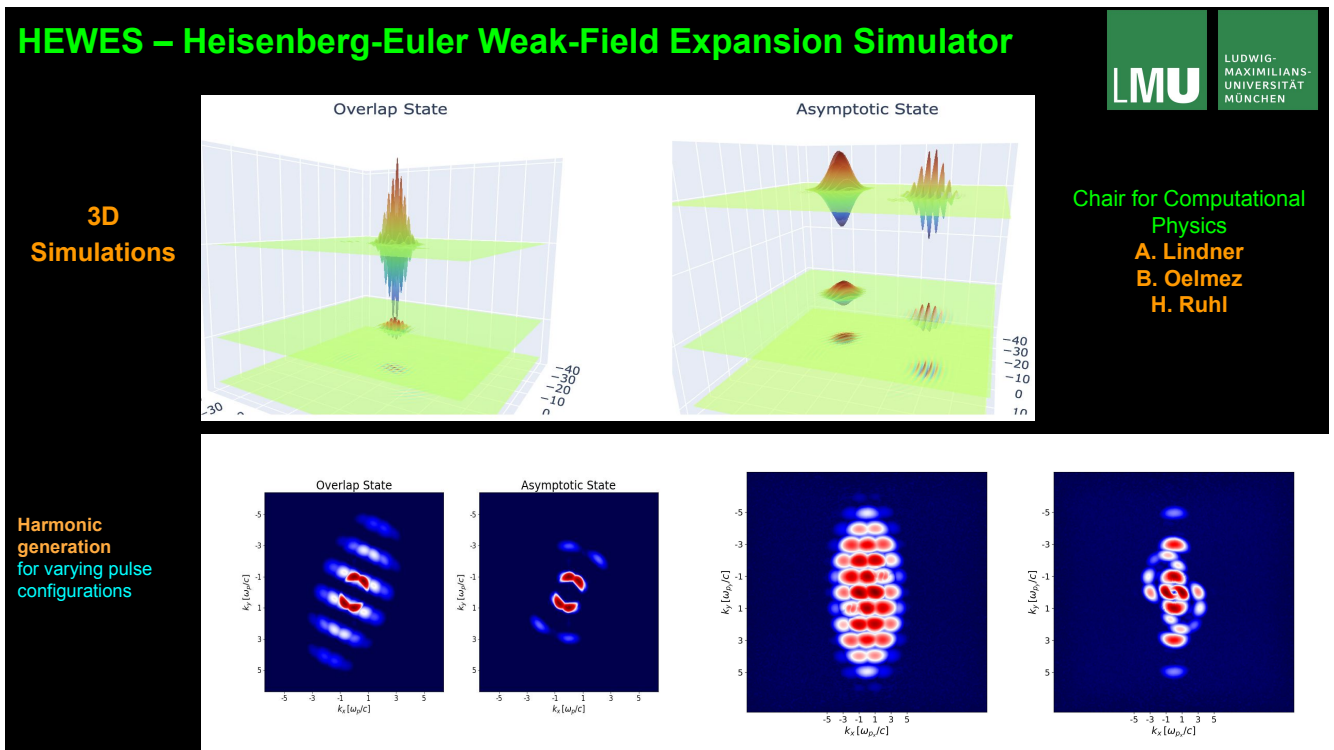


Figure 1: Graphical abstract.

*Email addresses:* [and.lindner@physik.uni-muenchen.de](mailto:and.lindner@physik.uni-muenchen.de) (Andreas Lindner),  
[b.oelmez@physik.uni-muenchen.de](mailto:b.oelmez@physik.uni-muenchen.de) (Baris Ölmez), [hartmut.ruhl@physik.uni-muenchen.de](mailto:hartmut.ruhl@physik.uni-muenchen.de) (Hartmut Ruhl)

## Highlights

- Inclusion of up to 6-photon processes in the Heisenberg-Euler weak-field expansion
- A universal 13th order of accuracy numerical scheme with a nonphysical modes filter
- Universality with respect to pulse configurations in contrast to analytical treatments
- Scalability on distributed computing systems
- Versatility in the context of high-precision experiments

### 1. Motivation and Significance

Most prominently, quantum electrodynamics (QED) is tested with collider experiments in the high-energy, low-intensity regime. Approaching the theory via the quantum vacuum tackles the low-energy, high-intensity regime that due to lack of high-intensity apparatuses has not been accessible thus far. Yet, this might as well be a portal towards new physics as the particle-antiparticle fluctuations flaring up in the vacuum consist of all existing particles [1, 2]. A currently hot topic is the anomalous magnetic moment of the Muon that quantum vacuum polarization is suspected to be a key factor contribution to [3].

The code presented here solves the nonlinear equations of the low-energy effective QED theory by Heisenberg and Euler [4]. The field of application is the quantum vacuum in the form of virtual electron-positron pairs (vacuum polarization) mediating nonlinear photon-photon interactions in the *effective* theory, thereby extending Maxwell's linear theory of electromagnetism. The corresponding effects, however, become noticeable only at high intensities of the involved light sources. Experimental and financial hurdles for their detection are thus very high. Facilities need to be equipped with high-intensity laser pulses and likewise ultra sensitive detectors. Advanced numerical frameworks to support research in this field with simulation data are required.

### 2. Theoretical Background

The Heisenberg-Euler Lagrangian [5] can be expanded in a weak-field form, where "weak" means below the *critical* field strength  $E_{cr} = \frac{m^2 c^3}{e\hbar} = 1.323 \times 10^{18} \frac{\text{V}}{\text{m}}$ , where  $e$  is the charge of the electron,  $m$  its mass,  $c$  the vacuum speed of light, and  $\hbar$  the reduced Planck constant. Electric fields with this intensity open up a new regime of strong-field QED, where the properties of the vacuum are substantially different [6, 5, 7]. The weak-field expansion of the Heisenberg-Euler Lagrangian can be written in terms of the electromagnetic invariants  $\mathcal{F}$  and  $\mathcal{G}$  defined by

$$\mathcal{F} = -\frac{c^2 F^{\mu\nu} F_{\mu\nu}}{4E_{cr}^2}, \quad \mathcal{G} = -\frac{c^2 F^{\mu\nu} F^*_{\mu\nu}}{4E_{cr}^2}. \quad (1)$$

The quantities  $F$  and  $F^*$  are the electromagnetic field-strength tensor and its dual. It is given by [8]

$$\mathcal{L}_{HE} \approx \frac{c^5 m^4}{360 \hbar^3 \pi^2} (4\mathcal{F}^2 + 7\mathcal{G}^2) \quad (2a)$$

$$+ \frac{c^5 m^4}{630 \hbar^3 \pi^2} (8\mathcal{F}^3 + 13\mathcal{F}\mathcal{G}^2) \quad (2b)$$

$$+ \frac{c^5 m^4}{945 \hbar^3 \pi^2} (48\mathcal{F}^4 + 88\mathcal{F}^2\mathcal{G}^2 + 19\mathcal{G}^4). \quad (2c)$$

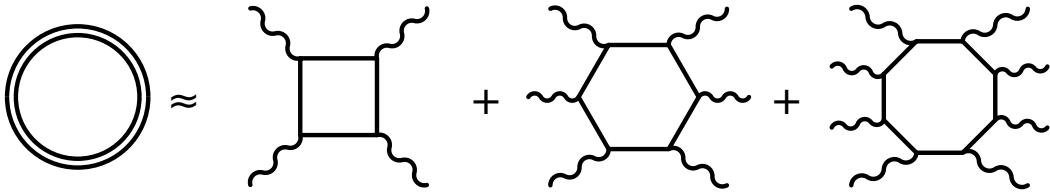


Figure 2: Depiction of the weak-field expansion of the Heisenberg-Euler Lagrangian. The double-lined loop to the left represents  $\mathcal{L}_{HE}$  while the diagrams to the right are the 4-, 6-, and 8-photon contributions due to the weak-field expansion of  $\mathcal{L}_{HE}$  corresponding to (2a),(2b), and (2c).

It solely depends on the electromagnetic invariants and subsequently (2a) is of the order  $\mathcal{O}((E/E_{cr})^4)$ . The effective interaction  $\mathcal{L}_{HE}$  can be graphically represented by a double-lined loop as in Figure 2 to the left. As a consequence, (2a) represents the four-photon contributions, (2b) the six-photon contributions, and (2c) the eight-photon contribution to the closed loop as illustrated in Figure 2.

### 3. Overview of the Implementation

The numerical simulation code presented in this work solves the weak-field expansion of the Heisenberg-Euler theory including up to 6-photon processes. The algorithm for solving the modified Maxwell equations is extensively discussed in [8]. Partial differential equations are turned into ordinary ones by means of a finite differences scheme on a discrete lattice. The devised scheme and the implementation work in one to three spatial dimensions plus time. Hyperparameter values at the user's option determine the overall accuracy. These are the order of the finite difference scheme – ranging from one to thirteen – the lattice resolution, and the error tolerances of the employed ODE solver. The *Sundials* [9] package is used for solving the arising system of nonlinear differential equations. Explicitly, the *CVode* solver from the *Sundials* family of solvers is employed, configured to use the Adams method (Adams-Moulton formula) [10] with a nonlinear solver implementation of a fixed-point iteration. Cluster computer communication for large-scale simulations with distributed memory is guided by the Message Passing Interface (*MPI*) [11] on a virtual Cartesian topology. The code is programmed in C++ with features up to the C++20 standard.

### 4. Usage

All high-level simulation settings are completely configurable in the main file.

1. The path where the output data is directed to is specified by the variable `outputDirectory`.
2. The decision whether to simulate in 1D, 2D, or 3D has to be made and only that full section uncommented. A screenshot of the 1D section is given in Figure 3.

It can then be specified

- the relative and absolute integration tolerances of the *CVode* solver. Recommended values are between 1e-12 and 1e-18.
- the order of accuracy of the numerical scheme via the stencil order. An integer in the range 1-13.
- the physical side lengths of the grid in meters.
- the number of lattice points per dimension.
- the slicing of the lattice into patches (only for 2D and 3D simulations, automatic in 1D) – this determines the number of patches and therefore the required distinct processing units for MPI. The total number of processes is given by the product of patches in any dimension.

Note: In the 3D case it should be insured that every patch is cubic in terms of lattice points. This is decisive for computational efficiency.

- whether to have periodic or vanishing boundary values (currently has to be chosen periodic).
  - whether you want to simulate on top of the linear vacuum only 4-photon processes (1), 6-photon processes (2), both (3), or none (0) – the linear Maxwell case.
  - the total time of the simulation in units  $c=1$ , i.e., the distance propagated by the light waves in meters.
  - the number of time steps that will be solved stepwise by CVode. In order to keep interpolation errors small, this number should not be chosen too small.
  - the multiple of steps at which the data has to be written to disk. The name of the files written to the output directory is of the form `{step_number}_{process_number}`.
    - which electromagnetic waveform(s) are to be propagated. It can be chosen between a plane wave (not much physical content, but useful for checks) and implementations of Gaussians in 1D, 2D, and 3D. Their parameters can be tuned. A description of the wave implementations is given in the code reference in the `docs` directory. Note that the 3D Gaussians, as they are implemented up to now, should be propagated in the `xy`-plane. More waveform implementations will follow in subsequent versions of the code.

3. The executable `Simulation` is built in the `src` directory issuing the `make` command. A skeleton Makefile is provided in the `src` directory of the software repository with the to-be-filled regions indicated.
4. The simulation is started. The number of processes is determined via the MPI execution command. Note that in 2D and 3D simulations this number has to coincide with the actual number of patches, as described above. Here, the simulation would be executed distributed over four processes:

```
mpirun -np 4 ./Simulation
```

5. Monitor `stdout` and `stderr`. The unique simulation identifier number (starting timestep = name of data directory), the process steps, and the used wall times per step are printed on `stdout`. Errors are printed on `stderr`. Note: Convergence of the employed CVode solver can not be guaranteed and issues of this kind can hardly be predicted. On top, they are even system dependent. Piece of advice: Only decimal numbers should be passed for the grid settings and initial conditions. CVode warnings and errors are reported on `stdout` and `stderr`. A `config.txt` file containing the relevant part of `main.cpp` is written to the output directory in order to save the simulation settings of each particular run.

Further notes and information on simulation settings, expected resource occupation, and the output analysis are listed in the `README` file of the project. There is also a doxygen-generated code reference. Jupyter notebooks with Python analysis examples are provided in the `examples` directory of the software repository.

## 5. Impact

Originating from a PhD project [12] the code is now being deployed for researcher usage.

In [8] various effects of nonlinear quantum vacuum theory have been demonstrated with simulations. These were successfully cross-checked against theoretical calculations, where available. Among these are of special interest in the community vacuum birefringence [13, 14, 15] and high-harmonic generation [16, 17]. The effective photon-photon interactions in these effects cause, during the collision of laser pulses, a rotation of the polarization direction and the arising of higher-frequency packets respectively. A selection of results on these effects are depicted in figures 4, 5, 6, 7. Some simulations in one spatial dimension can be cross-checked against analytical

```

////////// - 1D - //////////
/* A 1D simulation with specified */

/// Specify your settings here ///
constexpr array <sunrealtype,> CVodeTolerances={1.0e-16,1.0e-16}; /// - relative and absolute tolerances of the CVode solver
constexpr int StencilOrder=13; /// - accuracy order of the stencils in the range 1-13
constexpr sunrealtype physical_sidelength=300e-6; /// - physical length of the lattice in meters
constexpr sunintegertype latticepoints=6e3; /// - number of lattice points
constexpr bool periodic=true; /// - periodic or vanishing boundary values
int processOrder=3; /// - included processes of the weak-field expansion, see README.md
constexpr sunrealtype simulationTime=100.0e-6; /// - physical total simulation time
constexpr int numberOfSteps=100; /// - discrete time steps
constexpr int outputStep=100; /// - output step multiples

/// Add electromagnetic waves.
planewave plane1; /// A plane wave with
plane1.k = {1e5,0,0}; /// - wavevector (normalized to  $1/\lambda$ )
plane1.p = {0,0,0.1}; /// - amplitude/polarization
plane1.phi = {0,0,0}; /// - phase shift
planewave plane2; /// Another plane wave with
plane2.k = {-1e6,0,0}; /// - wavevector (normalized to  $1/\lambda$ )
plane2.p = {0,0,0.5}; /// - amplitude/polarization
plane2.phi = {0,0,0}; /// - phase shift
// Do not comment out this vector, even if no plane wave is used. But if, emplace used plane waves.
vector<planewave> planewaves;
//planewaves.emplace_back(plane1);
//planewaves.emplace_back(plane2);

gaussian1D gauss1; /// A Gaussian wave with
gauss1.k = {1.0e6,0,0}; /// - wavevector (normalized to  $1/\lambda$ )
gauss1.p = {0,0,0.1}; /// - polarization/amplitude
gauss1.x0 = {100e-6,0,0}; /// - shift from origin
gauss1.phig = 5e-6; /// - width
gauss1.phi = {0,0,0}; /// - phase shift
gaussian1D gauss2; /// Another Gaussian with
gauss2.k = {-0.2e6,0,0}; /// - wavevector (normalized to  $1/\lambda$ )
gauss2.p = {0,0,0.5}; /// - polarization/amplitude
gauss2.x0 = {200e-6,0,0}; /// - shift from origin
gauss2.phig = 15e-6; /// - width
gauss2.phi = {0,0,0}; /// - phase shift
// Do not comment out this vector, even if no Gaussian wave is used. But if, emplace used Gaussian waves.
vector<gaussian1D> Gaussians1D;
Gaussians1D.emplace_back(gauss1);
Gaussians1D.emplace_back(gauss2);

/// Do not change this below ///
int *interactions = &processOrder;
Sim1D(CVodeTolerances,StencilOrder,physical_sidelength,latticepoints,
      periodic,interactions,simulationTime,numberOfSteps,
      outputdirectory,outputStep,
      planewaves,Gaussians1D);
/////////

```

Figure 3: Excerpt of the main file. Shown is the section for 1D simulations that can be customized in the order listed in Section 4.

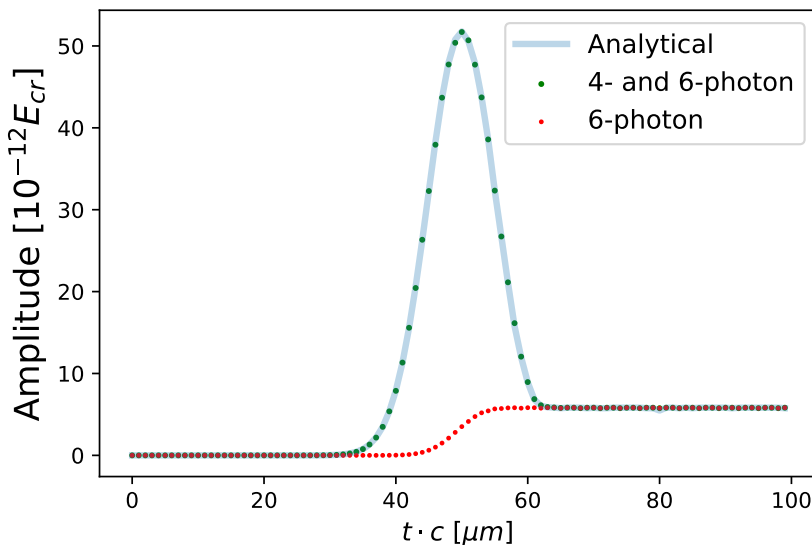


Figure 4: Time evolution of the amplitude of the second harmonic caused by nonlinear effects of a probe pulse colliding with a zero-frequency background pump in one dimension. Simulation results of [8] against the analytical solution obtained via [18].

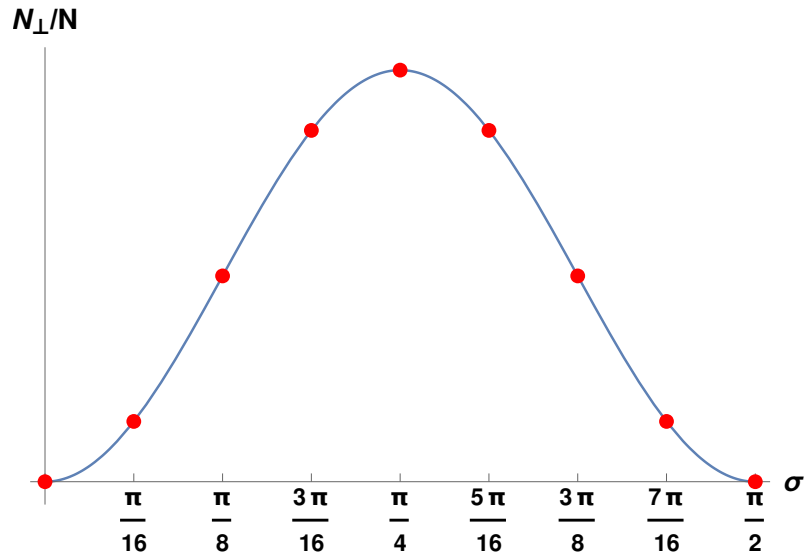


Figure 5: Polarization flipping ratio dependency on the relative polarization angle of probe and pump. Values obtained for specific pulse parameters in one spatial dimension given in [8]. Simulation results against the analytical solution obtained via [19].

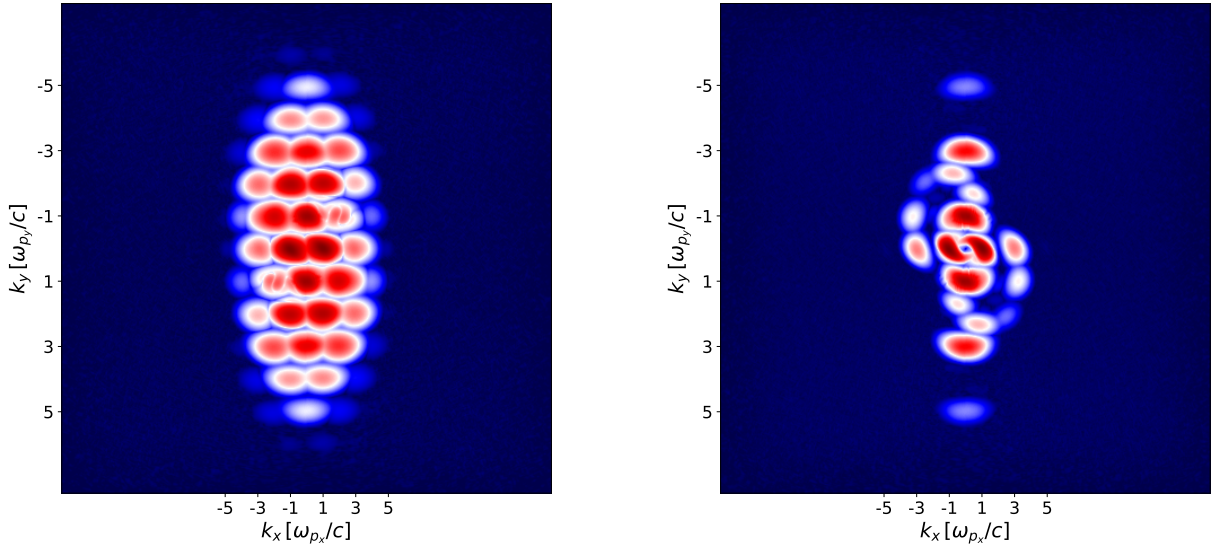


Figure 6: Generation of higher harmonics in two spatial dimensions. Shown are solely contributions from nonlinear effects. Perpendicularly colliding Gaussian pulses with different intensity and wavelength generate, e.g., a frequency spectrum during the interaction looking like corn (left) and asymptotic harmonics with a ying-yang-like structure in the center (right). The wavenumbers  $k$  denoting the axes are given in terms of the frequencies  $\omega$  of the involved pulses.

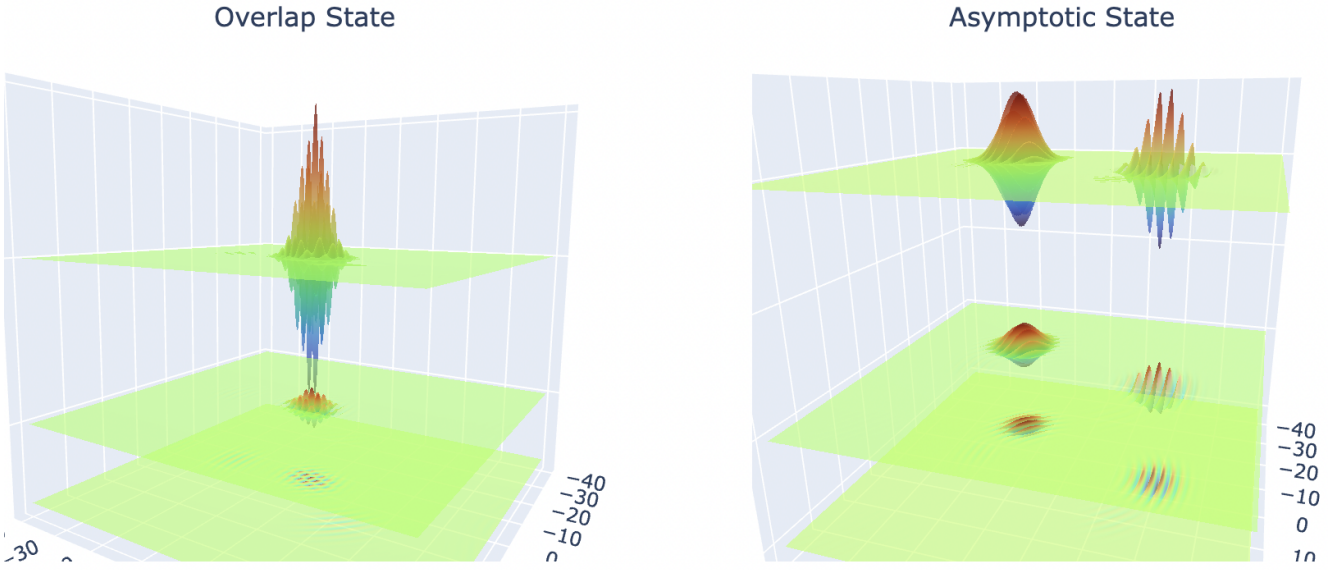


Figure 7: Visualization of a 3D simulation via hyperplanes at different vertical heights (polarization direction of the involved pulses). The distances in the horizontal planes are given in micro meters.

results. The figures for high harmonic generation in higher dimensions do not have analytical counterparts. In going to 3D, the code was running on thousands of cores simultaneously.

Theoretical setups are yet limited to special scenarios. Feasible calculations are constrained to simple configurations and arrangements of the involved laser pulses. Any such approximation in turn limits the accuracy of predictions and the precision with which theory can be tested [20]. The simulator is agnostic to the specific configuration. While theoretical calculations confine themselves to single effects, the solver takes into account the whole picture of the theory all at once. Furthermore, the solver is capable of time-resolving the processes, while theoretical approaches oftentimes concentrate on asymptotic values alone.

Only computer-driven approaches are flexible enough to accompany the development of experimental constructions and configurations.

A shift in perspective from limited analytical considerations to more versatile numerical solutions is apparent. There have been other approaches in the field: [21, 20] and [22]. The one presented in this work is currently the only one scalable on distributed computing systems. It stands out with a very high order of accuracy in the numerical scheme and the inclusion of six-photon processes and is thus extremely precise. The dispersion relation the algorithm delivers insures stability throughout the frequency spectrum and on top creates a benign imaginary part which annihilates nonphysical modes [8].

Research on the numerical side is intensified and ideas are being derived for going further in similar areas, driven by the success of this work. The development might go into further projects. One promising and important project is multi-scale simulation capability. This can be achieved by adaptive data structures and integrators combined with novel machine learning concepts.

The code has been refurbished and further developed as part of the DFG (German Research Foundation) Research Unit FOR 2783 "Probing the Quantum Vacuum at the High-Intensity Frontier". With the opening of this software its use can now become more widespread.

## Acknowledgments

The authors acknowledge the preliminary work by Arnau Pons Domenech. Together with Hartmut Ruhl, he developed the first code version and the underlying algorithm. Funding was provided by the Munich Cluster of Excellence (MAP), by the international Max-Planck Research School for Advanced Photonic Sciences (IMPRS-APS), by the Transregio TR-18

project B12, and the German Research Foundation (DFG) under Grant No. 416699545 within the Research Unit FOR 2783/1. Large parts of the computations during the production and verification process have been performed on the KSC cluster computing system of the Arnold Sommerfeld Center (ASC) for theoretical physics at LMU Munich, hosted at the Leibniz-Rechenzentrum (LRZ) in Garching and funded by the German Research Foundation (DFG) under project number 409562408.

## Data Statement

The raw simulation data used for this work amount to more than 100GB in size. It is archived on servers of the Arnold Sommerfeld Cluster (ASC) hosted by the Leibniz-Rechenzentrum (LRZ) in compliance with the regulations of the German Research Foundation (DFG).

## References

- [1] H. Gies, Strong laser fields as a probe for fundamental physics, *Eur. Phys. J. D* 55 (2009) 311–317. [arXiv:0812.0668](https://arxiv.org/abs/0812.0668), doi:10.1140/epjd/e2009-00006-0.
- [2] F. Karbstein, A. Blinne, H. Gies, M. Zepf, Boosting Quantum Vacuum Signatures by Coherent Harmonic Focusing, *Phys. Rev. Lett.* 123 (2019) 091802. doi:10.1103/PhysRevLett.123.091802.  
URL <https://link.aps.org/doi/10.1103/PhysRevLett.123.091802>
- [3] T. Blum, P. A. Boyle, V. GÜLPERS, T. Izubuchi, L. Jin, C. Jung, A. Jüttner, C. Lehner, A. Portelli, J. T. Tsang, Calculation of the hadronic vacuum polarization contribution to the muon anomalous magnetic moment, *Phys. Rev. Lett.* 121 (2018) 022003. doi:10.1103/PhysRevLett.121.022003.  
URL <https://link.aps.org/doi/10.1103/PhysRevLett.121.022003>
- [4] W. Heisenberg, H. Euler, Folgerungen aus der Diracschen Theorie des Positrons, *Zeitschrift für Physik* 98 (11) (1935) 714–732. doi:10.1007/BF01343663.  
URL <http://dx.doi.org/10.1007/BF01343663>
- [5] J. Schwinger, On Gauge Invariance and Vacuum Polarization, *Phys. Rev.* 82 (1951) 664–679. doi:10.1103/PhysRev.82.664.  
URL <https://link.aps.org/doi/10.1103/PhysRev.82.664>
- [6] F. Sauter, Über das verhalten eines elektrons im homogenen elektrischen feld nach der relativistischen theorie diracs, *Zeitschrift für Physik* 69 (11-12) (1931) 742–764.  
URL <https://link.springer.com/article/10.1007%2FBF01339461>
- [7] T. Heinzl, Strong-field qed and high-power lasers, *International Journal of Modern Physics A* 27 (15) (2012) 1260010. doi:10.1142/S0217751X1260010X.
- [8] A. Lindner, B. Ölmez, H. Ruhl, Numerical simulations of the nonlinear quantum vacuum in the heisenberg-euler weak-field expansion (2021). [arXiv:2109.08121](https://arxiv.org/abs/2109.08121).
- [9] A. C. Hindmarsh, P. N. Brown, K. E. Grant, S. L. Lee, R. Serban, D. E. Shumaker, C. S. Woodward, SUNDIALS: Suite of nonlinear and differential/algebraic equation solvers, *ACM Transactions on Mathematical Software (TOMS)* 31 (3) (2005) 363–396.
- [10] E. Hairer, S. P. Nørsett, G. Wanner, Solving ordinary differential equations. I, Nonstiff problems, Springer-Vlg, 1993.

- [11] L. Clarke, I. Glendinning, R. Hempel, The MPI message passing interface standard, in: Programming environments for massively parallel distributed systems, Springer, 1994, pp. 213–218.
- [12] A. Pons Domenech, Simulation of quantum vacuum in higher dimensions, Ph.D. thesis, lmu (2018).  
URL <https://edoc.ub.uni-muenchen.de/21885/>
- [13] J. Toll, The dispersion relation for light and its application to problems involving electron pairs, Ph.D. thesis, Princeton University, (unpublished) (1952).
- [14] R. Baier, P. Breitenlohner, The vacuum refraction index in the presence of external fields, *Il Nuovo Cimento B Series 10* 47 (1) (1967) 117–120. doi:10.1007/BF02712312.  
URL <http://dx.doi.org/10.1007/BF02712312>
- [15] T. Heinzl, B. Liesfeld, K.-U. Amthor, H. Schwoerer, R. Sauerbrey, A. Wipf, On the observation of vacuum birefringence, *Optics Communications* 267 (2) (2006) 318 – 321. doi:<http://dx.doi.org/10.1016/j.optcom.2006.06.053>.  
URL <http://www.sciencedirect.com/science/article/pii/S0030401806006481>
- [16] A. Fedotov, N. Narozhny, Generation of harmonics by a focused laser beam in the vacuum, *Physics Letters A* 362 (1) (2007) 1–5.  
URL <https://doi.org/10.1016/j.physleta.2006.09.085>
- [17] P. Böhl, B. King, H. Ruhl, Vacuum high-harmonic generation in the shock regime, *Phys. Rev. A* 92 (2015) 032115. doi:10.1103/PhysRevA.92.032115.  
URL <http://link.aps.org/doi/10.1103/PhysRevA.92.032115>
- [18] B. King, P. Böhl, H. Ruhl, Interaction of photons traversing a slowly varying electromagnetic background, *Phys. Rev. D* 90 (2014) 065018. doi:10.1103/PhysRevD.90.065018.  
URL <http://link.aps.org/doi/10.1103/PhysRevD.90.065018>
- [19] V. Dinu, T. Heinzl, A. Ilderton, M. Marklund, G. Torgrimsson, Vacuum refractive indices and helicity flip in strong-field QED, *Phys. Rev. D* 89 (2014) 125003. doi:10.1103/PhysRevD.89.125003.  
URL <http://link.aps.org/doi/10.1103/PhysRevD.89.125003>
- [20] A. Blinne, H. Gies, F. Karbstein, C. Kohlfürst, M. Zepf, All-optical signatures of quantum vacuum nonlinearities in generic laser fields, *Phys. Rev. D* 99 (2019) 016006. doi:10.1103/PhysRevD.99.016006.  
URL <https://link.aps.org/doi/10.1103/PhysRevD.99.016006>
- [21] H. Gies, F. Karbstein, C. Kohlfürst, All-optical signatures of strong-field qed in the vacuum emission picture, *Phys. Rev. D* 97 (2018) 036022. doi:10.1103/PhysRevD.97.036022.  
URL <https://link.aps.org/doi/10.1103/PhysRevD.97.036022>
- [22] T. Grismayer, R. Torres, P. Carneiro, F. Cruz, R. A. Fonseca, L. O. Silva, Quantum electrodynamics vacuum polarization solver, *New Journal of Physics* 23 (9) (2021) 095005. doi:10.1088/1367-2630/ac2004.  
URL <https://doi.org/10.1088/1367-2630/ac2004>

## Code Metadata

Code metadata description	Please fill in this column
Current code version	v0.2.0
Permanent link to code/repository used for this code version	<a href="https://gitlab.physik.uni-muenchen.de/ls-ruhl/hewes/-/tree/v0.2.0">https://gitlab.physik.uni-muenchen.de/ls-ruhl/hewes/-/tree/v0.2.0</a>
Legal Code License	BSD 3-Clause License
Code versioning system used	git
Software code languages, tools, and services used	C++, MPI, OpenMP, SUNDIALS
Compilation requirements, operating environments & dependencies	make
Link to code reference	<a href="https://gitlab.physik.uni-muenchen.de/ls-ruhl/hewes/docs/ref.pdf">https://gitlab.physik.uni-muenchen.de/ls-ruhl/hewes/docs/ref.pdf</a>
Support email for questions	and.lindner@physik.uni-muenchen.de